Available online at www.sciencedirect.com
SCIENCE DIRECT®
Journal of Chromatography A, 1047 (2004) 117–128
JOURNAL OF CHROMATOGRAPHY A
www.elsevier.com/locate/chroma

Evaluation of the analyses of *tert*-butyldimethylsilyl derivatives of naphthenic acids by gas chromatography–electron impact mass spectrometry

Joyce S. Clemente, Phillip M. Fedorak*

Department of Biological Sciences, University of Alberta, Edmonton, Alta., Canada T6G 2E9

Received 3 March 2004; received in revised form 16 June 2004; accepted 23 June 2004

Abstract

Naphthenic acids are a complex mixture of carboxylic acids with the general formula $C_nH_{2n+Z}O_2$ and they are natural, toxic components of crude oils. GC–MS analyses of *tert*-butyldimethylsilyl esters of naphthenic acids are used to estimate component distribution within naphthenic acids mixtures. Our evaluations of the GC–MS method showed that ions from column bleed erroneously appear as C14 $Z = -4$ acids and that correcting for heavy isotopes of C and Si do not significantly affect ion distribution plots. Overall, the GC–MS method appears to overestimate the relative proportion of low-molecular-mass acids.

Keywords: Derivatization, GC; Oil sands; Petroleum; Naphthenic acids; Butyldimethylsilyl esters; Organic acids

1. Introduction

Naphthenic acids are carboxylic acids with the general formula $C_nH_{2n+Z}O_2$ that are found in petroleum. Z is zero or a negative, even integer that specifies the hydrogen deficiency resulting from ring formation. An acylic compound has $Z = 0$, a single-ring compound has $Z = -2$, a two-ring compound has $Z = -4$, and so on. The acyclic components are highly branched [1]. High carboxylic acid concentrations in petroleum are the result of the deposit being immature, or because of incomplete bacterial degradation of the petroleum [2]. Naphthenic acids in crude oil cause processing equipment corrosion. This occurs in areas of high liquid flow velocity, in combination with temperatures between 220 and 400 °C [3,4].

Naphthenic acids in the Athabasca oil sands are released during the caustic, hot water extraction process used to recover bitumen from the oil sands [5]. The resulting extraction process wastewaters are stored in artificial ponds, such as the Mildred Lake Settling Basin (at Syncrude Canada Ltd.). These acids were determined to be the most toxic components of tailings water [6], and they have also been found to be toxic components in petroleum refinery effluents [7].

The structures of the components in naphthenic acids are related to their corrosivity [3], and their toxicity [8,9]. A wide variety of mass spectrometry (MS) methods have been used as a means of determining structural information about naphthenic acids. Ionization methods include electron impact [10–15], fast atom bombardment [16], chemical ionization [17,18], and electrospray ionization [1,19–22].

Of all the MS methods developed for naphthenic acids analysis, gas chromatography (GC)–electron impact MS analysis is likely the most accessible [14]. *N*-Methyl-*N*-(*tert*-butyldimethylsilyl)trifluoracetamide (MTBSTFA) has been used as a derivatizing agent to facilitate the analyses of naphthenic acids in commercial preparations [8,14,23] and in oil sands tailings ponds [8,23]. This method provides the same information as fluoride ion chemical ionization [14].

The observed masses can be organized into a two-dimensional matrix, where each cell corresponds to a carbon number, Z number combination [8,14]. Holowenko et al.

* Corresponding author. Tel.: +1 780 492 3670; fax: +1 780 492 9234.
E-mail address: phil.fedorak@ualberta.ca (P.M. Fedorak).

0021-9673/$ – see front matter © 2004 Elsevier B.V. All rights reserved.
doi:10.1016/j.chroma.2004.06.065

[8] plotted the relative intensities of these ions onto three-dimensional graphs as a means of better illustrating the differences in ion distributions by carbon and *Z* numbers. Variations of three-dimensional graphs representing naphthenic acids component distributions were also used by Rudzinski et al. [1], and Tomczyk et al. [15].

Our research group has a considerable amount of experience analyzing *tert*-butyldimethylsilyl derivatives of naphthenic acids by GC–MS in commercial preparations [8,23,24], in oil sands ores [23,25], in oil sands tailings waters [8] and in laboratory biodegradation studies [9]. In this paper, we present results from our evaluations of the method. Specifically, we assessed the order of elution of various components of a naphthenic acids sample and elucidated the characteristic appearance of contaminating GC column bleed. Six surrogate naphthenic acids were analyzed individually to determine the effects of stable isotopes and other fragmentation events on the parent ions. A mixture of these six compounds was then used to determine the efficiency of the derivatization reaction, ionization and detection. Finally, we corrected data for the stable heavy isotopes (^{13}C, ^{29}Si, and ^{30}Si) in the derivatized naphthenic acids samples, and determined the influence of these corrections on the distribution of ions in three-dimensional plots.

2. Materials and methods

2.1. Evaluation of the GC–MS method using model naphthenic acids

Six pure compounds (Fig. 1) were derivatized with MTBSTFA: 1-methyl-1-cyclohexanecarboxylic acid, *trans*-1,4-pentylcyclohexanecarboxylic acid, 2-hexyldecanoic acid (Aldrich, Milwaukee, WI, USA), eicosanoic acid (Applied Sciences Labs., State College, PA, USA), dicyclohexylacetic acid (Aldrich), and 5β-cholanic acid (Sigma, St. Louis, MO, USA). These were derivatized, and analyzed by GC–MS individually and in mixtures of all six surrogates. The resulting average mass spectra were studied to determine the influence of the other naturally occurring heavy isotopes of carbon (^{13}C), and silicon (^{29}Si and ^{30}Si) on the three-dimensional plots generated to summarize the distribution of naphthenic acids in a mixture.

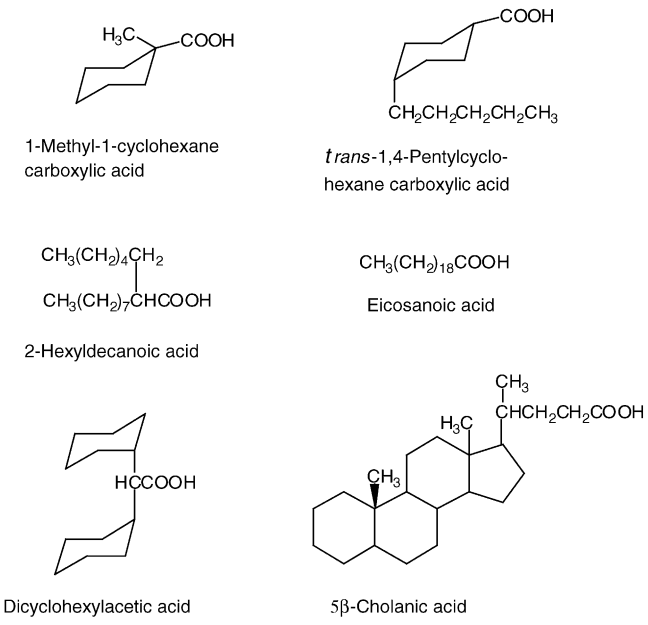

Fig. 1. Structures of surrogate naphthenic acid compounds used to determine the need for isotope correction.

High resolution MS analysis of *tert*-butyldimethylsilyl derivative of 5β-cholanic acid was performed using a Kratos MS50 mass spectrometer (Manchester, UK).

2.2. Assigning ions to be naphthenic acid

Any MS analysis of naphthenic acids yields a myriad of ions. To make sense of these data, the ions were assigned as naphthenic acids if they fit the empirical formula $C_nH_{2n+Z}O_2$ and the assumptions outlined [8]: (1) if $Z = -2$, one ring of at least five carbon atoms must be present in the molecule; (2) there must be one carbon atom available for the carboxyl group; (3) there must be at least one carbon atom available for an alkyl R group and, (4) structures with greater than three rings (i.e. $Z < -6$) may be fused on more than two sides.

Table 1 is an example of a matrix of the possible naphthenic acids within the carbon number range of 5–33, with 0–6 rings ($Z = 0$ to -12). The most abundant ion from the *tert*-butyldimethylsilyl derivative of naphthenic acid results from the loss of the *tert*-butyl group producing a base peak of $RCOOSi(CH_3)_2^+$, the [naphthenate + dimethylsilyl]$^+$ ion [14]. The masses shown in Table 1 are those [naphthenate + dimethylsilyl]$^+$ ions, and the empirical formulae shown are those of the naphthenic acids that would yield these ions after derivatization. We also refer to the [naphthenate + dimethylsilyl]$^+$ ions as the $[M + 57]^+$ ions, where *M* is the molecular mass of the corresponding naphthenic acid. Forty-seven entries in the top right side of Table 1 are boxed with a heavy border. Holowenko et al. [8] provide examples of why the 47 entries were excluded from being considered as naphthenic acids.

2.3. Correction for stable isotopes

The theoretical total ion intensity (I_T) of the [naphthenate + dimethylsilyl]$^+$ ion used to assign a compound to the corresponding carbon and *Z* numbers, is the sum of the observed ion intensity (I_M), the intensity of the $A + 1$ ion (I_{A+1}), and the intensity of the $A + 2$ ion (I_{A+2}). Ion distributions determined using the magnetic sector instrument, under low resolution MS were corrected for stable isotopes using the following equation:

$$I_T = I_M + I_{A+1} + I_{A+2} \quad (1)$$

Table 1
Expected carbon number (n) and Z number, based on nominal mass observed by MS of *tert*-butyldimethylsilyl derivatives, given the formula $C_nH_{2n+Z}O_2$

Carbon number	Z number						
	0	−2	−4	−6	−8	−10	−12
5	$C_5H_{10}O_2$[a] 159[b]	$C_5H_8O_2$ 157	$C_5H_6O_2$ 155	$C_5H_4O_2$ 153	$C_5H_2O_2$ 151	C_5O_2 149	–
6	$C_6H_{12}O_2$ 173	$C_6H_{10}O_2$ 171	$C_6H_8O_2$ 170	$C_6H_6O_2$ 168	$C_6H_4O_2$ 166	$C_6H_2O_2$ 164	C_6O_2 162
7	$C_7H_{14}O_2$ 187	$C_7H_{12}O_2$ 185	$C_7H_{10}O_2$ 183	$C_7H_8O_2$ 181	$C_7H_6O_2$ 179	$C_7H_4O_2$ 177	$C_7H_2O_2$ 175
8	$C_8H_{16}O_2$[c] 201	$C_8H_{14}O_2$ 199	$C_8H_{12}O_2$ 197	$C_8H_{10}O_2$ 195	$C_8H_8O_2$ 193	$C_8H_6O_2$ 191	$C_8H_4O_2$ 189
9	$C_9H_{18}O_2$ 215	$C_9H_{16}O_2$ 213	$C_9H_{14}O_2$ 211	$C_9H_{12}O_2$ 209	$C_9H_{10}O_2$ 207	$C_9H_8O_2$ 205	$C_9H_6O_2$ 203
10	$C_{10}H_{20}O_2$ 229	$C_{10}H_{18}O_2$ 227	$C_{10}H_{16}O_2$ 225	$C_{10}H_{14}O_2$ 223	$C_{10}H_{12}O_2$ 221	$C_{10}H_{10}O_2$ 219	$C_{10}H_8O_2$ 217
11	$C_{11}H_{22}O_2$ 243	$C_{11}H_{20}O_2$ 241	$C_{11}H_{18}O_2$ 239	$C_{11}H_{16}O_2$ 237	$C_{11}H_{14}O_2$ 235	$C_{11}H_{12}O_2$ 233	$C_{11}H_{10}O_2$ 231
12	$C_{12}H_{24}O_2$ 257	$C_{12}H_{22}O_2$ 255	$C_{12}H_{20}O_2$ 253	$C_{12}H_{18}O_2$ 251	$C_{12}H_{16}O_2$ 249	$C_{12}H_{14}O_2$ 247	$C_{12}H_{12}O_2$ 245
13	$C_{13}H_{26}O_2$ 271	$C_{13}H_{24}O_2$ 269	$C_{13}H_{22}O_2$ 267	$C_{13}H_{20}O_2$ 265	$C_{13}H_{18}O_2$ 263	$C_{13}H_{16}O_2$ 261	$C_{13}H_{14}O_2$ 259
14	$C_{14}H_{28}O_2$ 285	$C_{14}H_{26}O_2$ 283	$C_{14}H_{24}O_2$ 281	$C_{14}H_{22}O_2$ 279	$C_{14}H_{20}O_2$ 277	$C_{14}H_{18}O_2$ 275	$C_{14}H_{16}O_2$ 273
15	$C_{15}H_{30}O_2$ 299	$C_{15}H_{28}O_2$ 297	$C_{15}H_{26}O_2$ 295	$C_{15}H_{24}O_2$ 293	$C_{15}H_{22}O_2$ 291	$C_{15}H_{20}O_2$ 289	$C_{15}H_{18}O_2$ 287
16	$C_{16}H_{32}O_2$ 313	$C_{16}H_{30}O_2$ 311	$C_{16}H_{28}O_2$ 309	$C_{16}H_{26}O_2$ 307	$C_{16}H_{24}O_2$ 305	$C_{16}H_{22}O_2$ 303	$C_{16}H_{20}O_2$ 301
17	$C_{17}H_{34}O_2$ 327	$C_{17}H_{32}O_2$ 325	$C_{17}H_{30}O_2$ 323	$C_{17}H_{28}O_2$ 321	$C_{17}H_{26}O_2$ 319	$C_{17}H_{24}O_2$ 317	$C_{17}H_{22}O_2$ 315
18	$C_{18}H_{36}O_2$ 341	$C_{18}H_{34}O_2$ 339	$C_{18}H_{32}O_2$ 337	$C_{18}H_{30}O_2$ 335	$C_{18}H_{28}O_2$ 333	$C_{18}H_{26}O_2$ 331	$C_{18}H_{24}O_2$ 329
19	$C_{19}H_{38}O_2$ 355	$C_{19}H_{36}O_2$ 353	$C_{19}H_{34}O_2$ 351	$C_{19}H_{32}O_2$ 349	$C_{19}H_{30}O_2$ 347	$C_{19}H_{28}O_2$ 345	$C_{19}H_{26}O_2$ 343
20	$C_{20}H_{40}O_2$ 369	$C_{20}H_{38}O_2$ 367	$C_{20}H_{36}O_2$ 365	$C_{20}H_{34}O_2$ 363	$C_{20}H_{32}O_2$ 361	$C_{20}H_{30}O_2$ 359	$C_{20}H_{28}O_2$ 357
21	$C_{21}H_{42}O_2$ 383	$C_{21}H_{40}O_2$ 381	$C_{21}H_{38}O_2$ 379	$C_{21}H_{36}O_2$ 377	$C_{21}H_{34}O_2$ 375	$C_{21}H_{32}O_2$ 373	$C_{21}H_{30}O_2$ 371
22	$C_{22}H_{44}O_2$ 397	$C_{22}H_{42}O_2$ 395	$C_{22}H_{40}O_2$ 393	$C_{22}H_{38}O_2$ 391	$C_{22}H_{36}O_2$ 389	$C_{22}H_{34}O_2$ 387	$C_{22}H_{32}O_2$ 385
23	$C_{23}H_{46}O_2$ 411	$C_{23}H_{44}O_2$ 409	$C_{23}H_{42}O_2$ 407	$C_{23}H_{40}O_2$ 405	$C_{23}H_{38}O_2$ 403	$C_{23}H_{36}O_2$ 401	$C_{23}H_{34}O_2$ 399
24	$C_{24}H_{48}O_2$ 425	$C_{24}H_{46}O_2$ 423	$C_{24}H_{44}O_2$ 421	$C_{24}H_{42}O_2$ 419	$C_{24}H_{40}O_2$ 417	$C_{24}H_{38}O_2$ 415	$C_{24}H_{36}O_2$ 413
25	$C_{25}H_{50}O_2$ 439	$C_{25}H_{48}O_2$ 437	$C_{25}H_{46}O_2$ 435	$C_{25}H_{44}O_2$ 433	$C_{25}H_{42}O_2$ 431	$C_{25}H_{40}O_2$ 429	$C_{25}H_{38}O_2$ 427
26	$C_{26}H_{52}O_2$ 453	$C_{26}H_{50}O_2$ 451	$C_{26}H_{48}O_2$ 449	$C_{26}H_{46}O_2$ 447	$C_{26}H_{44}O_2$ 445	$C_{26}H_{42}O_2$ 443	$C_{26}H_{40}O_2$ 441
27	$C_{27}H_{54}O_2$ 467	$C_{27}H_{52}O_2$ 465	$C_{27}H_{50}O_2$ 463	$C_{27}H_{48}O_2$ 461	$C_{27}H_{46}O_2$ 459	$C_{27}H_{44}O_2$ 457	$C_{27}H_{42}O_2$ 455
28	$C_{28}H_{56}O_2$ 481	$C_{28}H_{54}O_2$ 479	$C_{28}H_{52}O_2$ 477	$C_{28}H_{50}O_2$ 475	$C_{28}H_{48}O_2$ 473	$C_{28}H_{46}O_2$ 471	$C_{28}H_{44}O_2$ 469
29	$C_{29}H_{58}O_2$ 495	$C_{29}H_{56}O_2$ 493	$C_{29}H_{54}O_2$ 491	$C_{29}H_{52}O_2$ 489	$C_{29}H_{50}O_2$ 487	$C_{29}H_{48}O_2$ 485	$C_{29}H_{46}O_2$ 483
30	$C_{30}H_{60}O_2$ 509	$C_{30}H_{58}O_2$ 507	$C_{30}H_{56}O_2$ 505	$C_{30}H_{54}O_2$ 503	$C_{30}H_{52}O_2$ 501	$C_{30}H_{50}O_2$ 499	$C_{30}H_{48}O_2$ 497
31	$C_{31}H_{62}O_2$ 523	$C_{31}H_{60}O_2$ 521	$C_{31}H_{58}O_2$ 519	$C_{31}H_{56}O_2$ 517	$C_{31}H_{54}O_2$ 515	$C_{31}H_{52}O_2$ 513	$C_{31}H_{50}O_2$ 511
32	$C_{32}H_{64}O_2$ 537	$C_{32}H_{62}O_2$ 535	$C_{32}H_{60}O_2$ 533	$C_{32}H_{58}O_2$ 531	$C_{32}H_{56}O_2$ 529	$C_{32}H_{54}O_2$ 527	$C_{32}H_{52}O_2$ 525
33	$C_{33}H_{66}O_2$ 551	$C_{33}H_{64}O_2$ 549	$C_{33}H_{62}O_2$ 547	$C_{33}H_{60}O_2$ 545	$C_{33}H_{58}O_2$ 543	$C_{33}H_{56}O_2$ 541	$C_{33}H_{54}O_2$ 539

Cells enclosed by heavy border represent theoretical compounds not considered naphthenic acids.
[a] Chemical formula corresponding to the expected mass.
[b] Expected formula mass for a compound with the corresponding carbon and Z numbers for the $[M + 57]^+$ ion, where M is the molecular mass of the underivatized acid.

where I_M is the observed ion intensity, I_{A+1} the intensity of the $A + 1$ ion, and I_{A+2} is the intensity of the $A + 2$ ion. The $A + 1$ ion occurs when there is one ^{13}C atom (1.07%) or one ^{29}Si atom (4.71%). The $A + 2$ ion occurs when there are two ^{13}C atoms, a combination of one ^{13}C and one ^{29}Si atom, or one ^{30}Si atom in the [naphthenate + dimethylsilyl]$^+$ ion. Using isotopic abundance from De Laeter [26], the probabilities can therefore be expressed as:

$$P_{A+1} = (0.0107 \times C_m) + (0.0471) \quad (2)$$

$$P_{A+2} = (0.0107 \times C_m)^2 + (0.031) + (0.047 \times 0.0107 \times C_m) \quad (3)$$

where P_{A+1} is the likelihood of getting the $A + 1$ ion, P_{A+2} is the likelihood of getting the $A + 2$ ion, and C_m is the number of carbon atoms in the [naphthenate + dimethylsilyl]$^+$ ion.

Substituting these expressions into Eq. (1) gives:

$$I_T = I_M + [(0.0107 \times C_m) + (0.0471)]I_T + [(0.0107 \times C_m)^2 + (0.031) + (0.047 \times 0.0107 \times C_m)]I_T \quad (4)$$

Eq. (4) shows that the intensity of the $A + 1$ and $A + 2$ ions are equivalent to the likelihood of those ions occurring, multiplied by the theoretical total intensity. The observed ion intensity (I_M), however, is the sum of the intensity of A, and $A + 2$ of an ion, with the same carbon number, but one less ring (i.e. $A - 2$). This term, must therefore be corrected as follows:

$$I_M = I_A - [(0.0107 \times C_m)^2 + (0.031) + (0.047 \times 0.0107 \times C_m)]I_{A-2} \quad (5)$$

where I_A is the intensity of the A ion (observed from MS), and I_{A-2} the intensity of the $A - 2$ ion (calculated).

Simplifying and rearranging Eq. (1), after substituting in Eqs. (2)–(5) results in Eq. (6):

$$I_T = \frac{I_A - [(0.0107 \times C_m)^2 + (0.031) + (0.047 \times 0.0107 \times C_m)]I_{A-2}}{0.922 - (0.0107 \times C_m)^2 - (0.0112 \times C_m)} \quad (6)$$

Eq. (6) was used to correct the ions observed in the three-dimensional graphs. Corrections were done only on samples discussed in Section 3.5.

2.4. Statistical analysis

A *t*-test method [23] was used to compare the results from GC–MS. For this analysis, the data in each matrix were divided into three groups: Group 1, carbon numbers 5–13, inclusive; Group 2, carbon numbers 14–21, inclusive; and Group 3, carbon numbers 22–33, inclusive.

2.5. GC–atomic emission detection (AED) analysis

A GC (HP 6890) system coupled to an atomic emission detector was used determine if the *tert*-butyldimethylsilyl derivatization efficiencies differed among the six surrogates. Two mixtures of the six acids were prepared and derivatized. These were analyzed by GC–MS and by GC–AED. The later analysis was performed using a temperature gradient of 10 °C min^{-1}, with an initial temperature of 40 °C and a final temperature of 300 °C. A 25 m methyl siloxane capillary column was used. The transfer line was held at 250 °C, and 1.5 μL of the sample was injected using the split injection mode. Helium was used as the carrier gas. Atomic emission of silicon was detected at 251.6 nm as in Kala et al. [27].

2.6. Naphthenic acids used for GC–MS studies

Five naphthenic acids extracts were used for these studies. These included an extract from the water in the Mildred Lake Settling Basin at Syncrude, designated MLSB7 [8], and naphthenic acids from three oil sands ores that were extracted as described by Holowenko et al. [8]. Two of the ore samples came from different locations at the Syncrude mines. These were designated Syncrude B (Basal ore) and Syncrude F (Syncrude North mine upper bench). The third ore sample came from the TrueNorth Energy LP lease. These sample were chosen because they contained C22 + naphthenic acids [8] (also designated Group 3 naphthenic acids by Clemente et al. [23]). The fifth naphthenic acids extract was obtained from three water samples taken from different locations along Beaver Creek on the Syncrude Lease. Each sample (500 mL) was acidified to pH 2.0–2.5 with 9 M H_2SO_4, and then extracted twice using two 20 mL portions of dichloromethane (Optima grade, Fisher Chemicals). The extracts were combined and then taken to dryness under a flow of compressed air because of the low concentrations of naphthenic acids in these samples. These were redissolved in a small volume of dichloromethane, combined and then taken to dryness before derivatizing for GC–MS analysis.

Refined Merichem naphthenic acids (a gift from Merichem Chemicals and Refinery Services, Houston, TX, USA) were also used for some studies.

2.7. Naphthenic acids derivatization and GC–MS

Naphthenic acids were derivatized using MTBSTFA which contained 1% *tert*-butyldimethylsilylchloride (Sigma) [14]. A modification of the method was that the reaction solution was dried under N_2 and dissolved to the original volume (100 μL) with dichloromethane. Samples (4 μL) were injected into a Varian Vista 6000 gas chromatograph fitted with a 30 m × 0.25 mm (film thickness: 0.25 μm) ZB5 column (Phenomenex, Torrance, CA, USA). The carrier gas was He and was set to maintain a capillary pressure of 10 psi. The initial temperature of 100 °C was held for 3 min, followed by an increase of 8 °C/min to a final temperature of 300 °C. The GC–MS transfer line was set at 290 °C and the VG 7070E magnetic sector mass spectrometer was operated in electron impact ionization mode to obtain mass spectra. A delay of 330 s was set so that the MS would remain off while the solvent eluted.

Spectral data were acquired using the Mass Spec Data System for Windows version 14.0c (Mass Spec Services, UK). Scan rate was 1.2 scan s^{-1} and the mass scan range was *m*/*z* 50–550. The MS collected mass values to 1 decimal place to prevent round-off errors due to drifts in the magnetic field. With the exception of the analysis of the Beaver Creek sample, the *m*/*z* values from the MS were truncated or rounded up, using the 0.7 amu cut-off point, to give nominal masses. Peak ion intensity values were averaged over the elution of the naphthenic acids hump, generally from retention time 10–35 or 40 min. The minimum occurrence variable for the averaged data was set at 1%, which meant an ion had to occur in at least 1% of the total scans averaged to be included in the final average data outputted from the computer. This was performed on all the data, except where it was indicated that 0% minimum occurrence was chosen. In the case where 0% was chosen, all of the scanned ions were included in the average. The averaged peak intensity values were inputted into a spreadsheet, which selected only those masses that corresponded to derivatized naphthenic acids with carbon numbers 5–33 and *Z* values from 0 to −12 (see Table 1).

3. Results and discussion

The analyses of naphthenic acids present three major challenges. First is characterizing the structures of the compounds in these complex, poorly defined mixtures. Second is determining the total concentration of naphthenic acids in a sample (such as oil or water), and third is ultimately determining the concentration of each individual acid in the mixture. Progress has been made toward meeting the second challenge through the development of GC [29] and HPLC [31] analytical methods. However, there is much work required to conquer the other two challenges. From literature, most effort has been directed toward the characterization of the compounds in naphthenic acids preparations. The work described in this report further assesses the use of a GC–MS method to characterize compounds in naphthenic acids, based on the carbon and *Z* numbers.

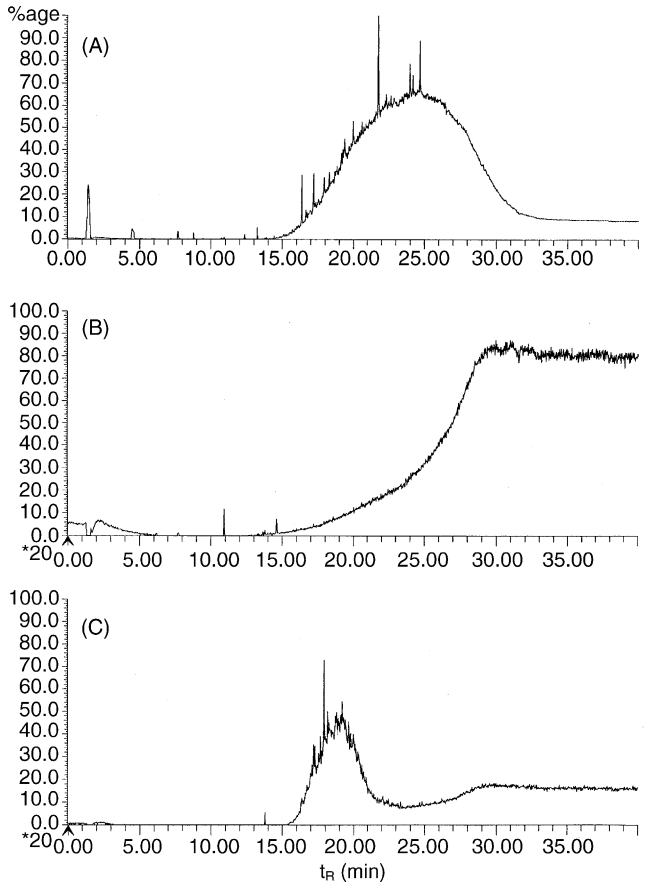

Fig. 2. GC–MS analysis of the derivatized naphthenic acids extracted from the Beaver Creek samples showing: (A) the total ion current, (B) the selected ion scan *m/z* 207 and (C) the selected ion scan *m/z* 281.

3.1. Elution of naphthenic acids and detection of GC column bleed

The derivatized naphthenic acids from the Beaver Creek sample were analyzed by GC–MS and the total ion current is shown in Fig. 2A. As observed by others [28,29], derivatized naphthenic acids eluted as an unresolved hump. The ion intensities were averaged over the retention time interval of 10–40 min, and the distribution of naphthenic acids is shown as a three-dimensional plot (Fig. 3A). These data were then re-analyzed averaging the peak ion intensities over 5 min intervals, and the distributions of naphthenic acids are summarized in Fig. 3B–F. In general, the abundance of higher molecular mass compounds increased as the retention time increased. For example, between 10 and 15 min (Fig. 3B), 82% of the ions corresponded to naphthenic acids with carbon numbers 9–12; between 15 and 20 min (Fig. 3C), 66% of the ions corresponded to naphthenic acids with carbon numbers 13–16; between 20 and 25 min (Fig. 3D) 52% of the ions corresponded to naphthenic acids with carbon numbers 15–18. After 30 min, the ion *m/z* 281 (corresponding to C14 $Z = -4$) became dominant (Fig. 3F), and between 35 and 40 min this ion accounted for 53% of the ions in the three-dimensional plot (data not shown).

This ion was traced to bleed from the GC column. Mass spectra collected after 35 min of GC analysis time showed major ions at *m/z* 207 (100% intensity), *m/z* 208 (21%), *m/z* 209 (13%), and *m/z* 281 (20%). Fig. 2B is the selective ion chromatogram for *m/z* 207, showing the increased column bleed after about 15 min, which reached a plateau at 30 min. Thus, the column bleed could also account for the appearance of the "naphthenic acids" that correspond to *m/z* 281 (e.g. the dominant peak at C14 $Z = -4$ in Fig. 3F). However, column bleed does not account for all of the C14 $Z = -4$ ions. Fig. 2C is the selective ion chromatogram for *m/z* 281, and it shows that a hump of these ions that eluted between 15 and 22 min, before the column bleed becomes very significant (Fig. 2B).

Fortuitously, the other three major ions from the column bleed do not affect the three-dimensional plots. Two of these ions, *m/z* 207 and 209, correspond to "naphthenic acids" with C9 $Z = -6$ and C9 $Z = -8$, respectively. As shown in Table 1, these fall into the boxed cells because they do not meet the criteria given by Holowenko et al. [8]. The third ion, *m/z* 208, has an even value, and all of the values considered to be [naphthenate + dimethylsilyl]$^+$ ions are odd (Table 1).

Experience has shown that heating the GC column at 360 °C for several hours before analyzing derivatized naphthenic acids virtually eliminates column bleed. As an added precaution, the column was also heated to 360 °C for 0.5 h each day before analyses started. However, when using this method, one must be wary of the appearance of a dominant ion corresponding to C14 $Z = -4$ (*m/z* 281) as shown in Fig. 3F. Although not previously reported, we have observed the C14 $Z = -4$ (*m/z* 281) ion as one of the most abundant ions from the analysis of heavily biodegraded naphthenic acids from laboratory cultures [9].

Surprisingly, Fig. 3E, corresponding to the derivatized naphthenic acids that had retention times of 25–30 min, showed the presence of low-molecular-mass "naphthenic acids" in the range of C5–C12. It seems unlikely that derivatized naphthenic acids in the range of C5–C12 would elute at about the same time as the high-molecular-mass compounds. The appearance of these low-molecular-mass "naphthenic acids" is likely due to misassigned fragments of [naphthenate + dimethylsilyl]$^+$ ions, as described in Section 3.3.

3.2. Ions originating from stable isotopes and loss of a methyl group

St. John et al. [14] studied the *tert*-butyldimethylsilyl derivatives of 1-methyl-1-cyclohexanecarboxylic acid and decanoic acid. They reported that the major advantage of producing the *tert*-butyldimethylsilyl derivatives of naphthenic acids for GC–MS analysis is that electron impact predominantly yields the [naphthenate + dimethylsilyl]$^+$ ions, with little other fragmentation to complicate assigning the acids to specific carbon and *Z* numbers. We explored this further, using the six surrogate naphthenic acids (Fig. 1 and Table 2). These acids were also used to determine the effects of sta-

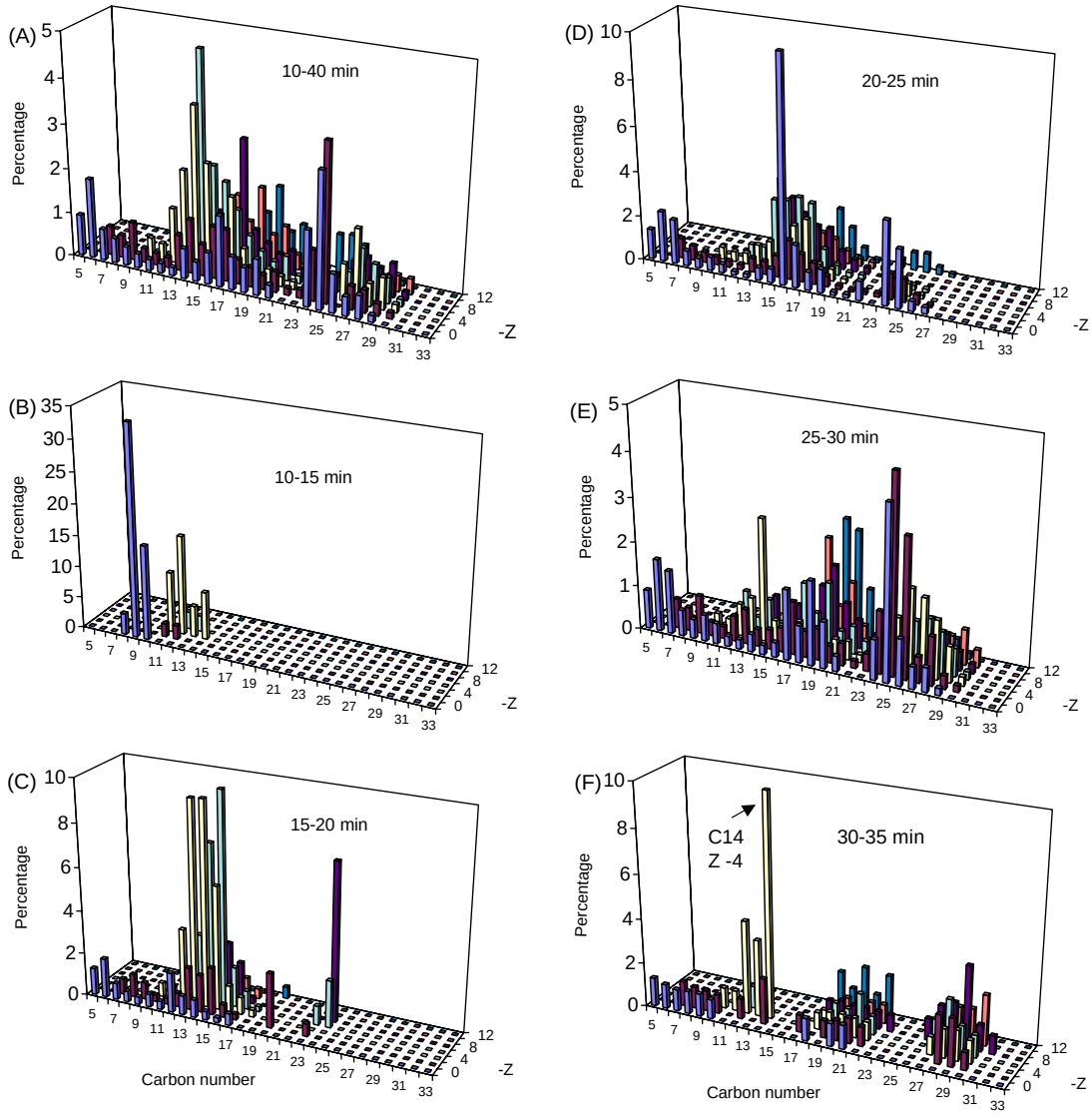

Fig. 3. Three-dimensional plots of data from GC–MS analysis of the derivatized naphthenic acids extracted from the Beaver Creek sample. Plots from peak ion intensity values averaged over the (min): (A) 10–40, (B) 10–15, (C) 15–20, (D) 20–25, (E) 25–30, and (F) 30–35.

ble isotopes on the intensities of ions observed in the three-dimensional plots produced after GC–MS analysis.

Fig. 4A shows the three-dimensional plot of 5β-cholanic acid after GC–MS analysis. Four ions were considered to be naphthenic acids by the spreadsheet used to assign ions to carbon numbers and Z values, and plot a three-dimensional graph. These had m/z values of 281, 417, 419, and 459 (Table 1). Three ions were from 5β-cholanic acid but the m/z 281 (C14 $Z = -14$) was from the GC column bleed (see Section 3.1). As shown in Fig. 4B, two of the ions (m/z = 417, and 459) were from different fragmentations of the derivative. Loss of the *tert*-butyl group, to give the [naphthenate + dimethylsilyl]$^+$ ion, was the major fragmentation giving m/z 417. This appears as the C24 $Z = -8$ peak in Fig. 4A. The loss of a methyl yields an ion of m/z 459, shown as the C27 $Z = -8$ peak in Fig. 4A. Fig. 4B shows the loss of a methyl group from the *tert*-methyl group, but the loss of any of the eight methyl groups could yield this ion. We use the term $[M + 99]^+$ ion to represent the ion formed when a methyl group is lost from the *tert*-butyldimethylsilyl derivative of a naphthenic acid. M represents the molecular mass of the naphthenic acid.

The $A + 2$ ion (A, a major ion, plus 2 Da [30]) was also detected because of the contributions of ^{13}C, ^{29}Si and ^{30}Si isotopes in the fragment ions of the *tert*-butyldimethylsilyl derivative of 5β-cholanic acid. The identity of the $A + 2$ ion was verified using high resolution MS, showing that the m/z 419 (nominal mass) ion in Fig. 4A (appearing as C24 $Z = -6$) was the $A + 2$ ion of the major ion m/z 417.

Ideally, the three-dimensional plot of a *tert*-butyldimethylsilyl derivative of a naphthenic acid would yield one column. However, there are three columns from the derivative of 5β-cholanic acid (Fig. 4A). The most abundant corresponds to the [naphthenate + dimethylsilyl]$^+$

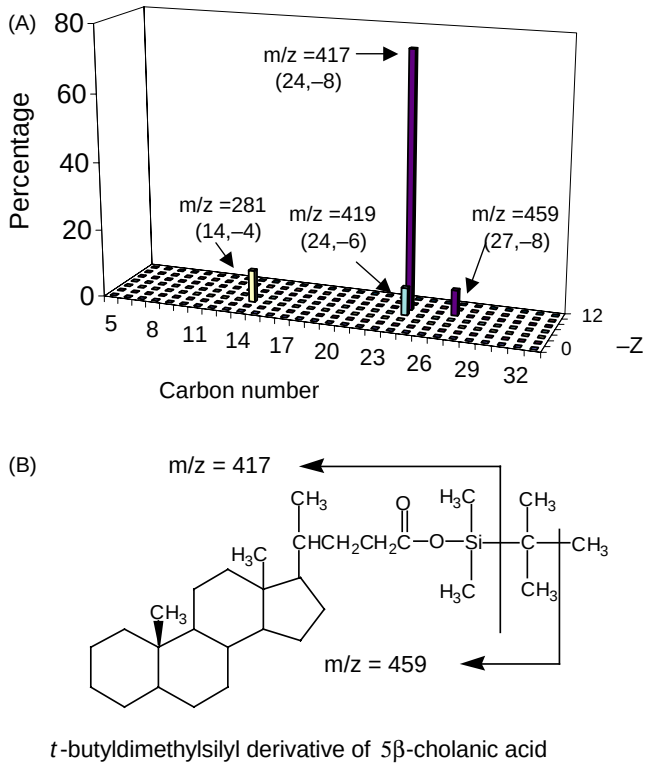

Fig. 4. Three-dimensional plot produced from the GC–MS analysis of the *tert*-butyldimethylsilyl derivative of: (A) 5β-cholanic acid and (B) the fragmentation of the derivative, where the *m/z* values are given for the naturally most abundant isotopes of C, H, and Si.

ion (*m/z* 417). One of the other ions (*m/z* 459) results from the loss of a methyl group, and the third ion (*m/z* 419) is the [naphthenate + dimethylsilyl]$^+$ ion that contains heavy isotopes of C and/or Si.

To further investigate the appearance these extra ions in the analysis of naphthenic acids, each of the six surrogates was derivatized and analyzed individually by GC–MS to determine the relative abundances of the $[M + 57]^+$, $A + 1$, $A + 2$, and the $[M + 99]^+$ ions. Table 2 summarizes the results of the relative abundances of the $[M + 57]^+$, $A + 2$, and $[M + 99]^+$ ions. In all but one case, the abundances were taken from the output of the spreadsheet that plots the three-dimensional graphs. The exception was the $A + 2$ ion from 2-hexyldecanoic acid, which has *m/z* 315 and falls into the boxed area of Table 1 (C17 $Z = -12$). Thus, the spreadsheet ignored this ion because it did not follow established definitions which distinguish naphthenic acids [8]. The relative abundances of this ion from 2-hexyldecanoic acid was calculated manually.

Consistent with a previous report [14], the [naphthenate + dimethylsilyl]$^+$ ion (the $[M + 57]^+$) ion was always the most abundant ion and can be used to assign the acid to appropriate carbon and *Z* numbers (Table 1). The relative abundances of these ions ranged from 59 to 89% (Table 2). The surrogates with the larger number of carbons (16, 20, and 24) yielded $[M + 57]^+$ ions with lower relative abundances (Table 2) than surrogates with lower carbon numbers (8, 12, and 14). In part, this could be predicted because the larger the number of carbon atoms, the greater the likelihood of ^{13}C being present, thereby yielding a more abundant $A + 1$ ion, diminishing the relative abundance of the $[M + 57]^+$ ion.

As shown in Table 2, these extra ions would make up a small percentage of the ions in the three-dimensional graph, with a minimum of 0% for the $[M + 99]^+$ ion of dicyclohexyl acetic acid and a maximum of 10% for the $A + 2$ ion of 2-hexyldecanoic acid. The sum of A, $A + 2$ and $[M + 99]^+$ ions was <100% because other minor ions, not considered in Table 2 were present.

3.3. Evaluating the GC–MS method with a mixture of six surrogate naphthenic acids

Fig. 5A shows the ideal three-dimensional plot from a hypothetical GC–MS analysis of the mixture of the six surrogates in solution at equimolar concentration. It shows that all the ions would have the same abundance (about 17%) if the yield of the derivatization reaction, the chromatography, and extent of fragmentation to give the [naphthenate + dimethylsilyl]$^+$ ions were the same.

Table 2
Summary of GC–MS analyses of the individual six pure acids with molecular formula $C_nH_{2n+Z}O_2$

Acid (C no., *Z* no.)	*A* ion $[M + 57]^+$ (*m/z*)	*A* ion $[M + 57]^+$ (%)[a]	$A + 2$ ion (*m/z*) (C no., *Z* no.)[b]	$A + 2$ ion (%)[a]	$[M + 99]^+$ (*m/z*) (C no., *Z* no.)[b]	$[M + 99]^+$ (%)[a]
1-Methyl-1-cyclo-hexanecarboxylic acid (8, −2)	199	86	201 (8, 0)	9	241 (11, −2)	3
trans-1,4-Pentyl-cyclohexanecarboxylic acid (12, −2)	255	84	257 (12, 0)	8	297 (15, −2)	2
Dicyclohexylacetic acid (14, −4)	281	89	283 (14, −2)	2	323 (17, −14)	0
2-Hexyldecanoic acid (16, 0)	313	72	315 (17, −12)[c]	10[c]	355 (19, 0)	3
Eicosanoic acid (20, 0)	369	59	371 (21, −12)	8	411 (23, 0)	2
5β-Cholanic acid (24, −8)	417	75	419 (24, −6)	8	459 (27, −8)	7

M is the molecular mass of the underivatized acid.
[a] Abundance of ion (%).
[b] C no. and *Z* no. assigned from Table 1 based on *m/z* value.
[c] This *m/z* value does not conform to the chemical definition of a naphthenic acid in [8].

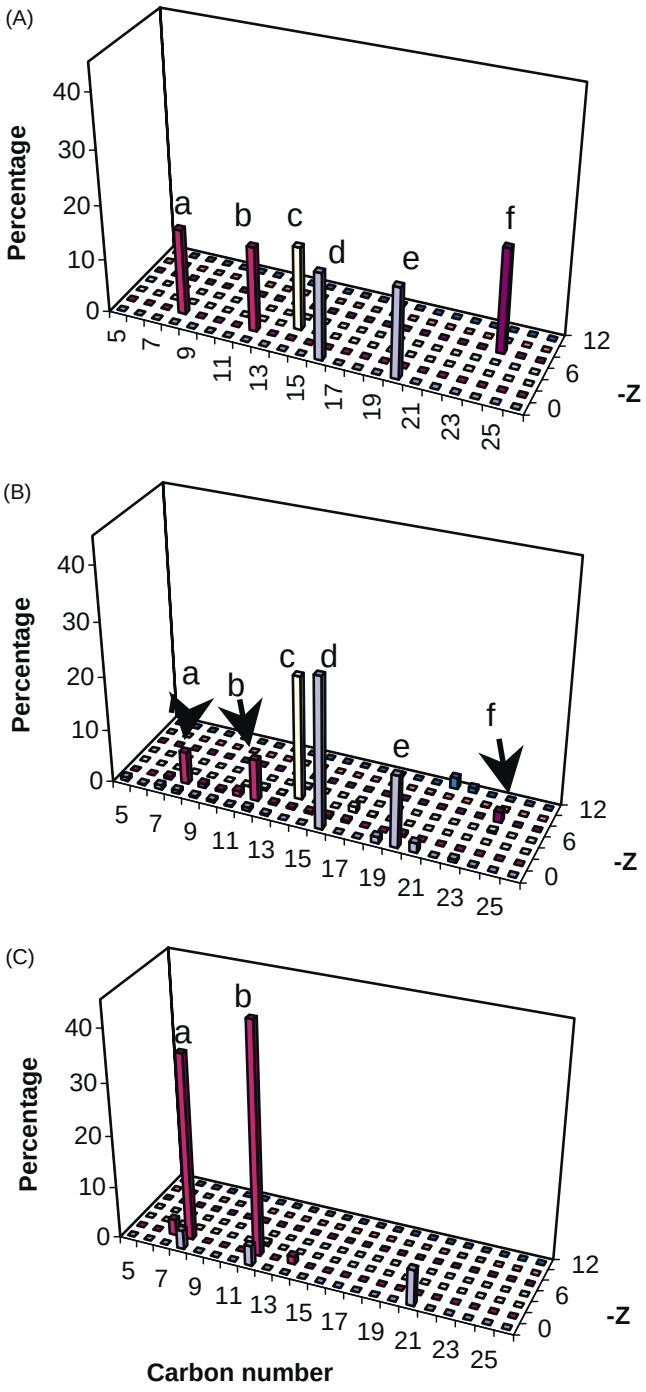

Fig. 5. Three-dimensional plots from the GC–MS analyses of *tert*-butyldimethylsilyl derivatives of the mixture of six surrogates containing equimolar concentrations: (A) ideal results; (B) actual results with the minimum occurrence variable for the averaged data was set at 0%; (C) actual results with the minimum occurrence variable for the averaged data was set at 1%. The mixture contained 400 μM each: (a) 1-methyl-1-cyclohexanecarboxylic acid; (b) *trans*-1,4-pentylcyclohexanecarboxylic acid; (c) dicyclohexaneacetic acid; (d) 2-hexyldecanoic acid; (e) eicosanoic acid; and (f) 5β-cholanic acid.

A mixture of the six surrogates, that contained nearly 400 μM of each acid, was derivatized and analyzed by GC–MS. Two three-dimensional plots of this mixture were produced. Fig. 5B shows the results when the mass spectrometry data were averaged specifying 0% minimum occurrence, and Fig. 5C shows the results when the mass spectrometry data were averaged specifying 1% minimum occurrence. These plot are markedly different from the ideal plot shown in Fig. 5A.

To determine whether the observed differences in ion intensities in Fig. 5B and C were due to the GC–MS analysis or the derivatization procedure, two near-equimolar mixtures of the six derivatized surrogates were analyzed by GC–AED, monitoring the emission from Si. If the derivatization efficiency was the same for each of the six surrogates, then an equal molar amount of Si would be detected for each derivatized compound. For each of the two mixtures, the GC–AED area count for each compound was divided by its micromolar concentration, and these six values were normalized by dividing them by the corresponding quotient obtained for 5β-cholanic acid. The mean normalized value was 1.09 and the standard deviation was 0.17. The highest normalized values were obtained for the most volatile compound (derivatized 1-methyl-1-cyclohexanecarboxylic acid). The normalized values for the derivatized 1-methyl-1-cyclohexanecarboxylic acid were 1.62 and 1.25 in each of the two mixtures. Excluding these two values from the calculation of the mean gave a value of 1.03 and a standard deviation of 0.05. These normalized results indicated that the efficiency of forming the *tert*-butyldimethylsilyl derivatives of each compound was essentially the same. Thus, the GC–MS analysis yielded the different ion abundance observed in Fig. 5B and C.

All six surrogates were well-separated and detected as sharp peaks in the total ion chromatogram, with retention times ranging from 10 to 35 min (data not shown). A total of 739 scans were taken between 10 and 35 min, and these were used to collect the average spectrum. When the data were averaged specifying 1% minimum occurrence each [naphthenate + dimethylsilyl]$^+$ ion had to occur in at least seven scans to be included in the average mass spectrum. However, because each compound eluted from the GC as a sharp peak, the corresponding [naphthenate + dimethylsilyl]$^+$ ion was observed in only a few scans so it was not included in the average mass spectrum or resulting three-dimensional plot (Fig. 5C). Only 1-methyl-1-cyclohexanecarboxylic acid (a) and *trans*-1,4-pentylcyclohexanecarboxylic acid (b) appeared in Fig. 5C. Selected ion monitoring showed that the characteristic ions for each of these compounds were present in the mass spectra of other compounds in the mixture. For example, the *m*/*z* 199 ion, corresponding to the [naphthenate + dimethylsilyl]$^+$ ion for 1-methyl-1-cyclohexanecarboxylic acid (a) was found as a fragment ion of the derivatives of dicyclohexylacetic (c), 2-hexyldecanoic (d), eicosanoic (e), and 5β-cholanic (f) acids. With the occurrence of the *m*/*z* 199 ion at various times in the chromatogram, the number of scans containing this ion exceeded the 1% minimum oc-

currence and *m*/*z* 199 was a dominant ion in the average spectrum.

When fragmentation of the [naphthenate + dimethylsilyl]$^+$ ions occurs, the fragments may be misassigned as a low-molecular-mass naphthenic acid if the new fragment masses fall into a cell in Table 1 (as is the case of the *m*/*z* 199 ions in the preceding paragraph). This leads to falsely high proportions of low-molecular-mass naphthenic acids in the three-dimensional plots, with corresponding falsely low proportions of high-molecular-mass naphthenic acids in these plots (because the sum of all the columns in a three-dimensional plot equals 100%).

Fig. 5B shows the three-dimensional plot of the same GC–MS analysis as Fig. 5C when the data were averaged specifying 0% minimum occurrence. In this case, ions in all of the scans were used for the average spectrum, and all six acids were detected. However, relative abundances ranged from only 2% for 5β-cholanic acid (f) to 28% for 2-hexyldecanoic acid (d). The reason for this wide range and the marked deviation from the ideal results (Fig. 5A) is not clear.

Several low-abundance columns are also observed in Fig. 5B. These would arise from other ions from the acids in the mixture. For example, ions (at about 1% abundance) were observed at C8 $Z = 0$, C12 $Z = 0$, and C21 $Z = -12$ in Fig. 5B. These correspond to the $A + 2$ ions of 1-methyl-1-cyclohexanecarboxylic, *trans*-1,4-pentylcyclohexanecarboxylic and eicosanoic acids, respectively, as shown in Table 2. Thus, as predicted from the analysis of 5β-cholanic acid (Fig. 4A), columns with carbon and *Z* numbers different from those expected for the surrogates in the mixture appeared in the three-dimensional plot (Fig. 5B).

The nominal mass of the [naphthenate + dimethylsilyl]$^+$ ion from derivatized dicyclohexylacetic is 281 (Table 2). This is the same mass as the C14 $Z = -4$ ion in Fig. 3F, caused by column bleed. This background ion typically gave *m*/*z* 280.7, which was truncated to 280, and the presence of this even mass ion was ignored (Table 1). Thus, the influence of column bleed was not seen in Fig. 5B and C.

3.4. Naphthenic acids analyses setting 0 or 1% minimum occurrence

The inability to detect four of the surrogates in Fig. 5C is disturbing, but it may not be an issue when analyzing an authentic naphthenic acids preparation. The four surrogates were not detected, when the data were averaged specifying 1% minimum occurrence for each [naphthenate + dimethylsilyl]$^+$ ion, because each compound eluted as a sharp peak and the ions occurred in <1% of the total scans. In contrast, an actual naphthenic acids preparation would very likely contain a large number of isomers of any given C and *Z* combination. These would all yield the same *m*/*z* value for a given $[M + 57]^+$ ion. The different isomers would elute at different retention times, and therefore, the $[M + 57]^+$ ions would appear in many different scans. These would be found in >1% of the total scans, thereby being detected when the data were averaged specifying 1% minimum occurrence. Fig. 2C is an example of how the $[M + 57]^+$ ions with *m*/*z* 281 were distributed in a hump that eluted between 15 and 22 min, increasing the probability of this mass occurring in >1% of the scans.

Four naphthenic acids preparations were analyzed by GC–MS and the average spectra obtained with 1 and 0% minimum occurrence were used to prepare three-dimensional plots. Fig. 6B and C show the comparisons of the results obtained from the TrueNorth sample. When compared by the statistical method of Clemente et al. [23], no differences were found between the data in these two plots. Similarly, no statistical differences were found after comparing the data from the 0 and 1% minimum occurrence averages for the following naphthenic acids preparations: Merichem, MLSB7, and Syncrude B ore sample.

We routinely use the 1% minimum occurrence variable because no background correction was done while analyzing the samples. It was assumed that the sample ions were eluting over an extended time period and that ions, which do not occur in at least 1% of the total ions scanned, are due to background noise.

3.5. Correction for stable isotopes

Table 3 summarizes the absolute and relative intensities of the A and $A + 1$ ions of the six pure acids used in this study. The last column of Table 3 shows that a significant proportion of the $[M + 57]^+$ ions from each compound appear as $A + 1$ ions because of the presence of isotopes such as ^{13}C or ^{29}Si. The occurrence of the $A + 1$ and $A + 2$ ions reduces the abundance of the $[M + 57]^+$ ion used to assign a compound to the corresponding carbon and *Z* numbers. This effect becomes more serious as molecular mass increases. Because of this, Eq. (6) was used to correct for the occurrence of the stable isotopes (^{13}C, ^{29}Si, and ^{30}Si).

The spreadsheet used by Holowenko et al. [8] considered only the most abundant isotopes (^{12}C and ^{28}Si). Other isotopes of these elements and their natural abundances are ^{13}C (1.07%), ^{29}Si (4.6832%) and ^{30}Si (3.0872%) [26].

The effects of the stable heavy isotopes are illustrated using the *tert*-butyldimethylsilyl derivative of 5β-cholanic acid (Fig. 4B) with carbon number 24 and $Z = -8$. The most abundant fragment of this compound is the [naphthenate + dimethylsilyl]$^+$ ion, arising from $^{12}C_{24}{}^{1}H_{39}{}^{16}O_2{}^{28}Si(^{12}C^{1}H_3)_2{}^+$ giving *m*/*z* 417. The *m*/*z* 417 ion in the average mass spectrum is considered to originate from a naphthenic acid with the formula $C_{24}H_{40}O_2$ (Table 1). This ion is designated the *A* ion in which the main elemental formula is composed of only the most abundant isotopes [30]. Four situations can occur that will reduce the abundance of the *A* ion in a three-dimensional plot.

First, if the *tert*-butyldimethylsilyl group contained ^{29}Si (which would occur in 4.6832% of the derivatized molecules) the resulting major fragment of the derivative would be $^{12}C_{24}{}^{1}H_{39}{}^{16}O_2{}^{29}Si(^{12}C^{1}H_3)_2{}^+$, which would give *m*/*z* 418.

Table 3
Summary of absolute and relative intensities of the selected ions from the GC–MS analyses of the individual six pure acids with molecular formula $C_nH_{2n+Z}O_2$

Acid (C no., *Z* no.)	*A* ion $[M + 57]^+$ (*m*/*z*)[a]	Intensity of the *A* ion	*A* + 1 ion (*m*/*z*)	Intensity of *A* + 1 ion	Relative intensity of *A* + 1 ion (%)[b]
1-Methyl-1-cyclo-hexanecarboxylic acid (8, −2)	199	182,000	200	35,000	19
trans-1,4-Pentyl-cyclohexanecarboxylic acid (12, −2)	255	405,000	256	70,000	17
Dicyclohexylacetic acid (14, −4)	281	1,048,000	282	91,000	9
2-Hexyldecanoic acid (16, 0)	313	471,040	314	119,000	25
Eicosanoic acid (20, 0)	369	232,000	370	68,000	29
5β-Cholanic acid (24, −8)	417	4000	418	1700	41

M is the molecular mass of the underivatized acid.
[a] These are the $[M + 57]^+$ ions entered in Table 1 used to assign carbon and *Z* numbers.
[b] 100 × (Intensity of *A* + 1 ion)/(intensity of *A* ion).

This is the *A* + 1 ion. There is no entry in Table 1 with a value of 418, so this ion is ignored by the spreadsheet. Thus, about 5% of the derivatized $^{12}C_{24}{}^{1}H_{40}{}^{16}O_2$ will not appear in the three-dimensional plot of the naphthenic acids distribution.

Second, if the organic acid contained one atom of ^{13}C (which would occur at a frequency of 1.07% per carbon atom in the molecule) the resulting major fragment of the derivative would be $^{13}C_1{}^{12}C_{23}{}^{1}H_{39}{}^{16}O_{22}{}^{8}Si(^{12}C^{1}H_3)_2{}^{+}$, which would give *m*/*z* 418. Again, there is no entry in Table 1 with a value of 418, and this ion is ignored. In this example, there are 24 carbon atoms, so the predicted abundance of this *A* + 1 ion is 24 × 1.07 or 26%. Thus, an additional 26% of the derivatized organic acids with the nominal formula $C_{24}H_{40}O_2$ would not appear in the three-dimensional plot depicting naphthenic acids distribution. The amount of error introduced by ignoring the *A* + 1 ion from ^{13}C increases with the number of carbon atoms in the naphthenic acid. Hence, the relative abundance of the high-molecular-mass naphthenic acids will be underestimated by the GC–MS method.

Third, if the *tert*-butyldimethylsilyl group contained ^{30}Si (which would occur in 3.0872% of the derivatized molecules) the resulting major fragment of the derivative would be $^{12}C_{24}{}^{1}H_{39}{}^{16}O_2{}^{30}Si(^{12}C^{1}H_3)_2{}^{+}$, which would give *m*/*z* 419 (the *A* + 2 peak ion). There is an entry in Table 1 with a value of 419, which is assigned as carbon number 24 *Z* = −6 (rather than −8). Thus, about 3% of the derivatized $^{12}C_{24}{}^{1}H_{40}{}^{16}O_2$ appears in the incorrect *Z* number in the three-dimensional plot of the naphthenic acids distribution.

Fourth, there is also a small probability that the organic acid may contain two heavy isotopes, such as two ^{13}C atoms. The magnitude of this effect increases as the number of carbon atoms in the organic acid increase. This would produce a molecular ion that is two mass units higher than expected (i.e. an *A* + 2 ion) if only ^{12}C atoms are considered. There could also be one ^{13}C atom and one ^{29}Si atom, again yielding an *A* + 2 ion. These different combinations of isotopes would be expected to occur for each of the [naphthenate + dimethylsilyl]$^+$ entries in Table 1.

The spreadsheet [8] was modified to calculate the abundance of each [naphthenate + dimethylsilyl]$^+$ ion using Eq. (6). Fig. 6A and B compare the three-dimensional plots from the GC–MS analysis of the derivatized naphthenic acids from the TrueNorth ore sample, with and without correction for the heavy isotopes. Table 4 shows the uncorrected, and corrected ion abundance for TrueNorth sample, and for the naphthenic acids from three other sources. The ions in each sample are grouped by carbon number [23], and the relative abundance of the ions (%) in each group was summed.

Table 4
Comparison of naphthenic acid ion distributions according to carbon numbers, without (uncorrected), and with (corrected) correction for stable isotopes

Naphthenic acids from	Group based on C no.	Sums[a] (%)		*P*[b]
		Uncorrected	Corrected	
TrueNorth	C5–C13	16.9	15.1	0.388
	C14–C21	66.4	65.8	0.950
	C22+	16.8	19.0	0.448
MLSB7	C5–C13	20.7	18.8	0.639
	C14–C21	60.2	58.6	0.928
	C22+	19.0	22.6	0.525
Syncrude B	C5–C13	15.9	14.7	0.601
	C14–C21	78.5	78.8	0.988
	C22+	5.6	6.5	0.454
Syncrude E	C5–C13	22.0	20.4	0.710
	C14–C21	71.2	71.7	0.976
	C22+	6.9	7.9	0.541

[a] Sum of all ions in the specified group.
[b] *P*-value from *t*-test [23].

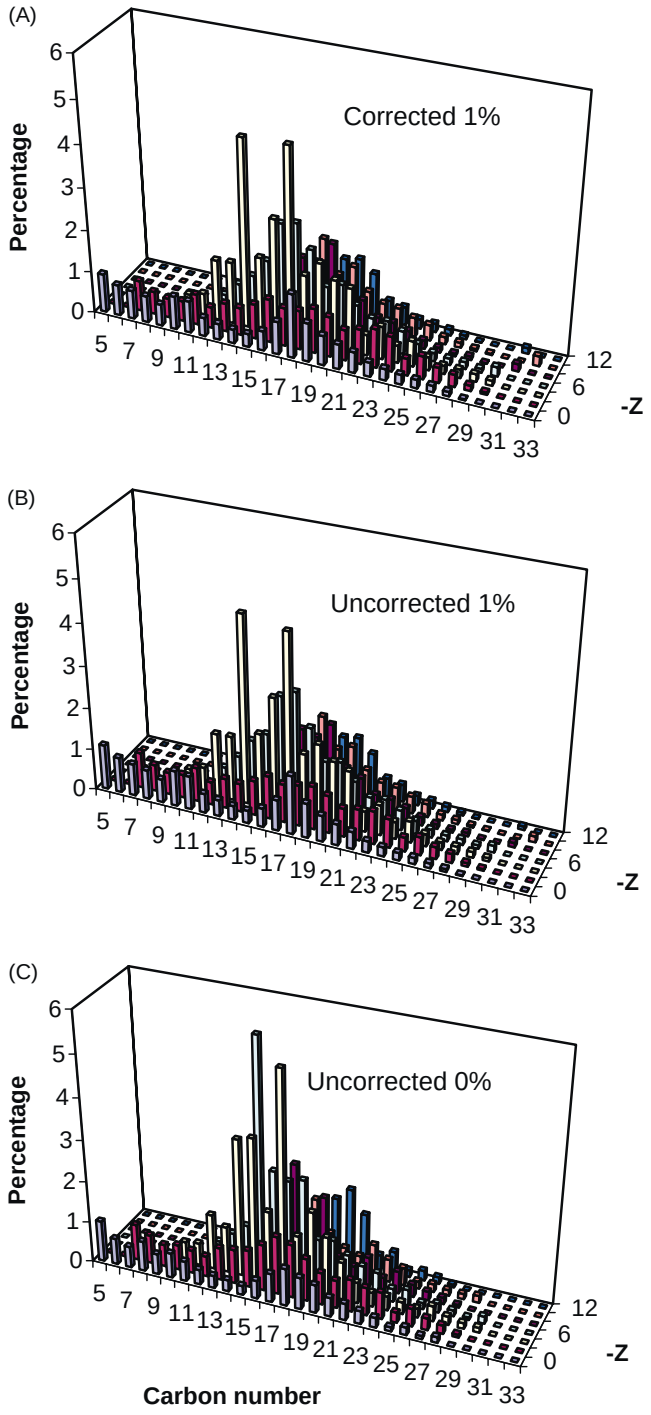

Fig. 6. Three-dimensional plots of data from GC–MS analysis of the derivatized naphthenic acids from the TrueNorth showing the distribution of ions: (B and C) without correction for heavy isotopes and (A) with correction for heavy isotopes by applying Eq. (6) to each combination of carbon and *Z* numbers shown in Table 1. The minimum occurrence variable for the averaged data was set at 1% (A and B) or 0% (C).

In the corrected data, the most noticeable differences in these sums were a decrease in the relative abundance of the low-molecular-mass acids (C5–C13) (Table 4). This is because the isotope correction increases the relative abundance of the higher molecular mass acids. This is best seen in the increase in the abundance of the acids in the C22+ group (Table 4). Of course, for each sample, the total of the three group sums is 100% (except for some round-off error).

The uncorrected values were compared to the corrected values using a *t*-test [23] to determine if the distributions changed as a result of correcting for heavy isotopes. The results in Table 4 showed that there was no statistically significant difference in the distribution of ions ($P < 0.05$) in any of the groups of any of the four naphthenic acids samples.

St. John et al. [14] and Lo et al. [32] briefly discussed the effects of heavy isotopes, but they did not correct their data for these isotopes. Applying Eq. (6) to correct for heavy isotopes made only small, statistically insignificant changes to the distributions of ions in four naphthenic acids samples (Table 4).

4. Conclusions

The GC–MS method has been used to characterize naphthenic acids from various sources [8,14,23] and to follow the changes in naphthenic acids composition during biodegradation [9]. This investigation has provided new insights into the results obtained from the GC–MS analyses of *tert*-butyldimethylsilyl derivatives of naphthenic acids. Like all other currently available methods for naphthenic acids analyses, the GC–MS method has its limitations. For example, some ions are misassigned because of unexpected cleavage or the presence of heavy isotopes, and this leads to overestimation of the abundance of low-molecular-mass naphthenic acids. Despite its limitations, the GC–MS method is very useful for the analyses of naphthenic acids, but researchers using this method must be aware of its limitations, and must be careful not to over-interpret data collected from these analyses.

The GC–MS method does not provide quantitative results, and the three-dimensional graphs must not be mistaken to be quantitative. These provide convenient, qualitative "fingerprints" of naphthenic acids, based on the relative abundance of the ions detected by MS that can be used to compare different naphthenic acids preparations.

Acknowledgements

Funding for this project was provided by Syncrude Canada Ltd., Suncor Energy Inc., TrueNorth Energy LP, Albian Sands Energy, Canadian Natural Resources Limited, and the Canadian Water Network. We thank L. Harrower and R. Whittal in the Mass Spectrometry Laboratory in the Department of Chemistry for their assistance throughout the project. W. Marsh prepared and analyzed the Beaver Creek samples, and M. Morphy did GC–AED analyses. We gratefully acknowledge the continuing support and interest in this work provided by Dr. M. MacKinnon of Syncrude Canada Ltd.

References

[1] W.E. Rudzinski, L. Oehlers, Y. Zhang, Energy Fuels 16 (2002) 1178.
[2] B.P. Tissot, D.H. Welte, Petroleum Formation and Occurrence, Springer, New York, 1978.
[3] A. Turnbull, E. Slavcheva, B. Shone, Corrosion 54 (1998) 922.
[4] R.D. Kane, M.S. Cayard, Mater. Perform. 38 (7) (1999) 48.
[5] L.L. Schramm, E.N. Stasiuk, M. MacKinnon, in: L.L. Schramm (Ed.), Surfactants, Fundamentals and Applications in the Petroleum Industry, Cambridge University Press, UK, 2000, p. 365.
[6] R.E.A. Madill, M. Orzechowski, G. Chen, B.G. Brownlee, N.J. Bunce, Environ. Toxicol. 16 (2001) 197.
[7] D.C.L. Wong, R. van Compernolle, J.G. Nowlin, D.L. O'Neal, G.M. Johnson, Chemosphere 32 (1996) 1669.
[8] F.M. Holowenko, M.D. MacKinnon, P.M. Fedorak, Water Res. 36 (2002) 2843.
[9] J.S. Clemente, M.D. MacKinnon, P.M. Fedorak, Environ. Sci. Technol. 38 (2004) 1009.
[10] W.K. Seifert, R.M. Teeter, Anal. Chem. 41 (1969) 786.
[11] W.K. Seifert, R.M. Teeter, W.G. Howells, M.J.R. Cantow, Anal. Chem. 41 (1969) 1638.
[12] V.G. Lebedevskaya, Y.S. Brodskii, L.M. Saltykova, Petrol. Chem. -Engl. Tr. 17 (3) (1978) 187.
[13] J.B. Green, S.K.-T. Yu, R.P. Vrana, J. High Resolut. Chromatogr. 17 (1994) 427.
[14] W.P. St. John, J. Righani, S.A. Green, G.D. McGinnis, J. Chromatogr. A 807 (1998) 241.
[15] N.A. Tomczyk, R.E. Winans, J.H. Shinn, R.C. Robinson, Energy Fuels 15 (2001) 1498.
[16] T. Fan, Energy Fuels 5 (1991) 371.
[17] I. Dzidic, A.C. Somerville, J.C. Raia, H.V. Hart, Anal. Chem. 60 (1988) 1318.
[18] C.S. Hsu, G.J. Dechert, W.K. Robbins, E.K. Fukuda, Energy Fuels 14 (2000) 217.
[19] K. Qian, W.K. Robbins, C.A. Hughey, H.J. Cooper, R.P. Rodgers, A.G. Marshall, Energy Fuels 15 (2001) 1505.
[20] V.V. Rogers, K. Liber, M.D. MacKinnon, Chemosphere 48 (2002) 519.
[21] M.P. Barrow, L.A. McDonnell, X. Feng, J. Walker, P.J. Derrick, Anal. Chem. 75 (2003) 860.
[22] W. Gabryelski, K.L. Froese, Anal. Chem. 75 (2003) 4612.
[23] J.S. Clemente, N.G.N. Prasad, M.D. MacKinnon, P.M. Fedorak, Chemosphere 50 (2003) 1265.
[24] F.M. Holowenko, M.D. MacKinnon, P.M. Fedorak, Water Res. 35 (2001) 2595.
[25] J.S. Clemente, M.Sc. Thesis, University of Alberta, Edmonton, 2004.
[26] J.R. De Laeter, Pure Appl. Chem. 63 (1991) 991.
[27] S.V. Kala, E.D. Lykissa, R.M. Lebovitz, Anal. Chem. 69 (1997) 1267.
[28] D.C. Herman, P.M. Fedorak, M. MacKinnon, J.W. Costerton, Can. J. Microbiol. 35 (1994) 467.
[29] D.M. Jones, J.S. Watson, W. Meredith, M. Chen, B. Bennett, Anal. Chem. 73 (2001) 703.
[30] F.W. McLafferty, Interpretation of Mass Spectra, third ed., University Science Books, Mill Valley, CA, 1980.
[31] T.-W. Yen, W.P. Marsh, M.D. MacKinnon, P.M. Fedorak, J. Chromatogr. A 1033 (2004) 83.
[32] C.C. Lo, B.G. Brownlee, N.J. Bunce, Anal. Chem. 75 (2003) 6394.